Computational Materials Science 47 (2009) 128–134

Contents lists available at ScienceDirect

Computational Materials Science

journal homepage: www.elsevier.com/locate/commatsci

An improved technique for the solution of edge crack problem for finite plate

Y.Z. Chen *, X.Y. Lin, Z.X. Wang

Division of Engineering Mechanics, Jiangsu University, Zhenjiang, Jiangsu 212013, People's Republic of China

ARTICLE INFO

Article history:
Received 1 May 2009
Received in revised form 28 June 2009
Accepted 30 June 2009
Available online 26 July 2009

Keywords:
Edge crack
Stress intensity factor
T-stress
Complex potentials
Numerical solution

ABSTRACT

This paper provides a detailed examination for the edge crack problem of finite plate. The Williams expansion for the crack problem is used first. Secondly, the complex potentials for the central crack problem are used in the present study, which is called the improved technique hereafter. In both techniques, the eigenfunction expansion variational method (EEVM) is used for evaluating the undetermined coefficients in the expansion form. The ratio of height versus width of plate (h/w) is varying from 1.5, 1.0, 0.75, 0.5, 0.4, 0.3 to 0.25. The ratio of edge crack length versus width of plate (a/w) takes two sets: (1) $a/w = 0.1$, 0.2,… to 0.9, (2) $a/w = 0.01$, 0.02,… to 0.09. The detailed computation proves that for moderate cases of the a/w ratio, for example, $0.2 < a/w < 08$, the deviations for SIFs and *T*-stress from two techniques are minor. However, for the case of short edge crack length, for example, $a/w < 0.05$, the deviations for SIFs and *T*-stress from two techniques are significant. It is found that the Williams expansion may not be suitable for the short edge crack, for example, $a/w < 0.05$.

1. Introduction

Williams investigated the stress distribution near a crack tip [1]. In the Williams expansion, the first two terms are relating to the stress intensity factors. The third term is denoted as the *T*-stress and can be regarded as the stress acting parallel to the crack flanks [2].

Since the edge crack specimen is generally used in experiment, the edge crack problems were investigated by many researchers [3–9]. The stress intensity factors (SIFs) and the *T*-stress are values to be evaluated in the problems.

A variety of methods was used to solve the edge crack problem for finite plate. The elastic *T*-stress at the tip of a mixed mode crack can be determined by the so-called second order weight functions through a work-conjugate integral [3]. The *T*-stress in an edge cracked rectangular plate is evaluated on the boundary collocation method, which is based on the Williams expansion at the vicinity of crack tip. Formulation of the Green's function is suggested. The undetermined coefficients in the Green's function can be determined by some typical boundary value problems [4,5].

A simple method, called the stress difference method, is proposed to compute the elastic *T*-stress at a crack tip [6]. In the method, the difference between two stress components at a point ahead of the crack tip is demonstrated to be able to evaluate the elastic *T*-stress efficiently and accurately. In the study, the ranges of a/w (edge crack length/width of plate) are within 0.2–0.8.

Finite element analyses have been conducted to calculate the *T*-stress for an edge cracked plate [7,8]. The studied problems were within the ranges $0.2 < a/w < 0.8$. A simple formula for obtaining the elastic *T*-stress in boundary element method fracture mechanics analysis is presented [9]. This formula is obtained by comparing the variation of the displacements along the quarter-point crack-tip element with the classical field solution for the crack-tip.

If the boundary collocation method (BCM) is used in the crack problems, one may be concerned about the influence of the used boundary collocation scheme to the computed result. For example, it was said, "the reason for the difference in stability of various boundary collocation procedure is not clear" [10]. Moreover, it was pointed out that the boundary collocation method (BCM) is quite sensitive to the distribution of collocation points and may give unstable results [8].

Recently, a derivation of the Green's function for the Laplace equation for an annular region by using the Trefftz method was suggested [11]. In the derivation, the first part solution in the Green's function can be obtained from a singular solution for the Laplace equation. In addition, the second part solution is a harmonic function in the annular region. The second part may be expressed in different forms. One possibility is to express the second part in the form of a series ([11] Eqs. (15) and (16)). Another possibility is to express second part in a combination of many harmonic functions caused by many image sources outside the annular region. The boundary value, for example in the Dirichlet problem, caused by the first part is just compensated by those by the second part. In the Trefftz method, the assumed function generally satisfies the Laplace equation. However, it does not satisfy the boundary conditions.

* Corresponding author. Tel.: +86 0511 88780780; fax: +86 0511 88791739.
E-mail address: chens@ujs.edu.cn (Y.Z. Chen).

0927-0256/$ - see front matter © 2009 Elsevier B.V. All rights reserved.
doi:10.1016/j.commatsci.2009.06.023

Comparing with the Trefftz method used in an annular region [11], similar situation happens in the edge crack problem. There are several ways to express the stress field in the edge crack problem. The Williams expansion is one way to express the stress filed. Alternatively, the complex potentials for the central crack problem are used in the present study, which is another way to model the stress field in the edge crack problem.

In this paper, the eigenfunction expansion variational method (Abbreviated as EEVM) is developed to evaluate the stress intensity factor and the T-stress in the crack problem [12,13]. In the EEVM, the computation does not depend on the boundary collocation scheme. In addition, the EEVM has a clear physical meaning. The EEVM is actually equal to the least potential energy principle in elasticity.

It was found from references that many researchers devoted their efforts to the favorable conditions, for example, the ratios a/w (edge crack length/width of plate) are within in the range 0.2–0.8. In addition, a few cases were devoted to study the serious conditions, for example, $a/w < 0.05$.

This paper provides a detailed examination for edge crack problem for finite plate. The Williams expansion for the crack problem is used first. Secondly, the complex potentials in the central crack problem are used in the present study, which is called the improved technique hereafter [12,13]. In both techniques, the EEVM is used for evaluating the involved undetermined coefficients. The ratio for height versus width of plate (h/w) is varying from 1.5, 1.0, 0.75, 0.5, 0.4, 0.3 and 0.25. The ratio for edge crack length versus width of plate (a/w) takes two sets: (1) a/w = 0.1, 0.2,… to 0.9, (2) a/w = 0.01, 0.02,… to 0.09. This is to say cases of comparative short edge crack are also studied in this paper. The SIFs and the T-stress are computed from two techniques.

The properties of the complex potentials used in two techniques are analyzed. It is found that the first two terms in complex potentials relating to Williams expansion are lacking of some basic stress field at the remote place, for example, the tension stress in y-direction. To overcome this inconvenient condition, it is suggested to use the complex potentials from a central crack in the present study. The detailed computation proves that for moderate cases of the a/w ratio, for example, $0.2 < a/w < 08$, the deviations for SIFs and T-stress from two techniques are minor. However, in the case of short edge crack length, for example, $a/w < 0.05$, the deviations for SIFs and T-stress from two techniques are significant. It is found that the Williams expansion may not be suitable for the short edge crack, for example, $a/w < 0.05$.

2. Analysis

2.1. Solution of the edge crack problem for a finite plate using Williams expansion form

The complex variable function method plays an important role in plane elasticity. Fundamental of this method is introduced. In the method, the stresses (σ_x, σ_y, σ_{xy}), the resultant forces (X, Y) and the displacements (u, v) are expressed in terms of complex potentials $\phi(z)$ and $\psi(z)$ such that [14]

$$\sigma_x + \sigma_y = 4\mathrm{Re}\Phi(z),$$

$$\sigma_y - \sigma_x + 2i\sigma_{xy} = 2[\bar{z}\Phi'(z) + \Psi(z)], \quad (1)$$

$$f = -Y + iX = \phi(z) + z\overline{\phi'(z)} + \overline{\psi(z)}, \quad (2)$$

$$2G(u + iv) = \kappa\phi(z) - z\overline{\phi'(z)} - \overline{\psi(z)}, \quad (3)$$

where $\Phi(z) = \phi'(z)$, $\Psi(z) = \psi'(z)$, a bar over a function denotes the conjugated value for the function, G is the shear modulus of elasticity, $\kappa = (3 - \nu)/(1 + \nu)$ in the plane stress problem, $\kappa = 3 - 4\nu$ in the plane strain problem, and ν is the Poisson's ratio. Sometimes, the displacements u and v are denoted by u_1 and u_2, the stresses σ_x, σ_y and σ_{xy} by σ_1, σ_2 and σ_{12}, the coordinates x and y by x_1 and x_2.

From the traction free condition along the edge crack and Eq. (2) (Fig. 1), the following condition is obtainable

$$\left(\phi(z) + z\overline{\phi'(z)} + \overline{\psi(z)}\right)_{x<0 y=0^{\pm}} = 0. \quad (4)$$

From condition Eq. (4), we will obtain the following complex potentials [15]

$$\phi(z) = \sum_{k=1}^{M} A_k z^{k/2} \quad (\text{where } A_k = A_{k,re} + iA_{k,im}), \quad (5)$$

$$\psi(z) = \sum_{n=1}^{M} D_k z^{k/2}, \quad (6)$$

where

$$D_k = -\frac{1}{2}(kA_k + 2(-1)^k \overline{A}_k). \quad (7)$$

The complex potentials shown by Eqs. (5) and (6) are actually the Williams expansion form in the edge crack problem [1].

Behaviors of the first two terms in the complex potentials are listed in Table 1. It is seen from the listed results that the first two terms can model the singular character of stresses at the crack tip zone (Fig. 1). However, they can only model the stress state $\sigma_x = c$, $\sigma_y = 0$, $\sigma_{xy} = 0$ at the remote zone. From the tabulated results we find that the first two terms in the Williams expansion form

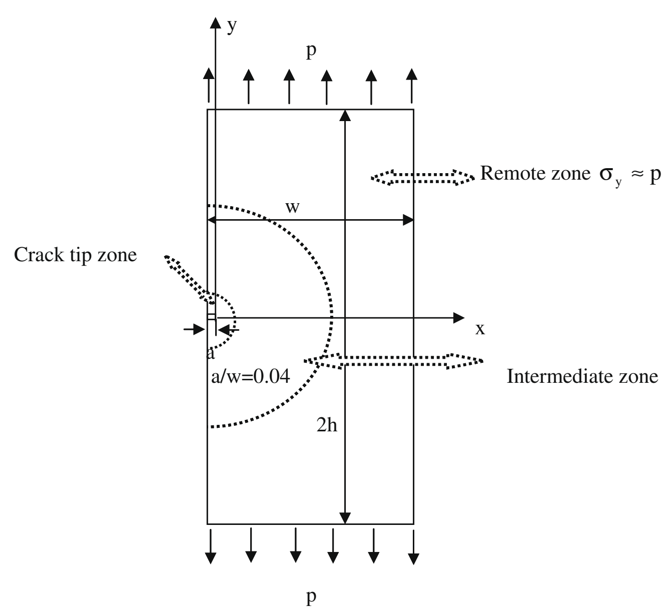

Fig. 1. A rectangular plate with a short length crack in tension p.

Table 1
Behaviors of the first two terms in the complex potentials defined by Eqs. (5) and (6).

	$A_1 = 1$	$A_1 = i$	$A_2 = 1$	$A_2 = i$
The behavior of the first two terms at the crack tip zone				
σ_x	Singular stress	Regular stress	4	0
σ_y	Singular stress	Regular stress	0	0
σ_{xy}	Regular stress	Singular stress	0	0
The behavior of the first two terms at remote zone $\lvert z\rvert \gg a$ with $r = \lvert z\rvert$				
	$A_1 = 1$	$A_1 = i$	$A_2 = 1$	$A_2 = i$
σ_x	$O(r^{-1/2})$	$O(r^{-1/2})$	4	0
σ_y	$O(r^{-1/2})$	$O(r^{-1/2})$	0	0
σ_{xy}	$O(r^{-1/2})$	$O(r^{-1/2})$	0	0

cannot provide the following stress states: (1) $\sigma_x = 0$, $\sigma_y \approx c$, $\sigma_{xy} = 0$, (2) $\sigma_x = 0$, $\sigma_y = 0$, $\sigma_{xy} \approx c$, at the remote place (Fig. 1). However, in a real edge crack problem in tension shown by Fig. 1, the stress state is dominated by $\sigma_x = 0$, $\sigma_y = p$, $\sigma_{xy} = 0$ at the remote zone. This is a particular disadvantage to use the Williams expansion in the short edge crack case.

The variational principal is suggested to solving the edge crack problem. In the solution, we can let

$$X_{2k-1} = A_{k,re}, \quad X_{2k} = A_{k,im} \quad (k = 1, 2, \dots M). \tag{8}$$

The variational principal of elasticity leads to the following algebraic equation [12,13]

$$\sum_{k=1}^{2M} P_{mk} X_k = Q_m \quad (m = 1, 2, \dots 2M), \tag{9}$$

where

$$P_{mk} = P_{km} = \int_C u_i^{(m)} \sigma_{ij}^{(k)} n_j \, ds \quad (m, k = 1, 2, \dots 2M), \tag{10}$$

$$Q_m = \int_C u_i^{(m)} \bar{p}_i \, ds \quad (m = 1, 2, \dots 2M), \tag{11}$$

where "C" denotes the boundary of the cracked plate, $\bar{p}_i$ is the traction applied on the boundary. $u_i^{(m)}$ is the displacement from mth term in the expansion, $\sigma_{ij}^{(k)}$ is the stress from kth term in the expansion, and n_j is the direction cosine.

After the algebraic Eq. (9) is solved, the SIFs, or $K_1 - iK_2$ can be obtained from

$$K_1 - iK_2 = \lim_{z \to 0} 2\sqrt{2\pi z}\,\phi'(z) = \sqrt{2\pi}(A_{1,re} + iA_{1,im}). \tag{12}$$

From the front position method suggested in [16], the T-stress can be defined by

$$T = -\lim_{z \to 0} \mathrm{Re}(\sigma_y - \sigma_x + 2i\sigma_{xy}) = -2 \lim_{z \to 0} \mathrm{Re}(\bar{z}\phi''(z) + \psi'(z)). \tag{13}$$

In Eq. (13), z is a real and $z > 0$. From Eqs. (10) and (13), we have

$$T = 4A_{2,re}. \tag{14}$$

2.2. Solution of the edge crack problem for a finite plate using an improved technique

The edge crack problem can be considered as a particular problem of the center crack problem [12,13]. Thus, the complex potentials for the center crack problem are introduced below. The configuration for the problem is indicated in Fig. 2, and the loading may be a simple tension in y-direction.

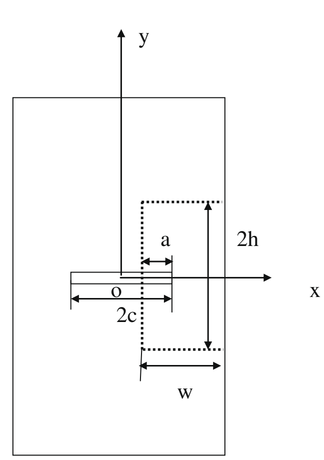

Fig. 2. An edge crack plate cut from a rectangular plate with a central crack.

In the derivation, a substitution for complex potential is defined as follows [15]:

$$\psi(z) = \bar{\omega}(z) - z\phi'(z). \tag{15}$$

After using this substitution, Eqs. (1)–(3) are converted into

$$\begin{aligned} &\sigma_x + \sigma_y = 4\mathrm{Re}\Phi(z), \\ &\sigma_y - \sigma_x + 2i\sigma_{xy} = -2(\Phi(z) + (z - \bar{z})\Phi'(z) - \overline{\Omega}(z)), \end{aligned} \tag{16}$$

$$f = -Y + iX = \phi(z) + (z - \bar{z})\overline{\phi'(z)} + \omega(\bar{z}), \tag{17}$$

$$2G(u + iv) = \kappa\phi(z) - (z - \bar{z})\overline{\phi'(z)} - \omega(\bar{z}), \tag{18}$$

where $\Omega(z) = \omega'(z)$.

From the traction free condition along the crack face, an expansion form for the complex potentials was suggested previously [12,13]

$$\phi(z) = \phi_1(z) + \phi_2(z), \quad \omega(z) = \omega_1(z) + \omega_2(z), \tag{19}$$

$$\phi_1(z) = \omega_1(z) = \sum_{k=1}^{N} E_k X(z) z^{k-1} \quad (\text{where } E_k = E_{k,re} + iE_{k,im}), \tag{20}$$

$$\phi_2(z) = -\omega_2(z) = \sum_{k=1}^{N} F_k z^k \quad (\text{where } F_k = F_{k,re} + iF_{k,im}), \tag{21}$$

where $X(z)$ is a function defined by

$$X(z) = \sqrt{z^2 - c^2} \quad (\text{taking the branch } \lim_{z \to \infty} X(z)/z = 1). \tag{22}$$

In the suggested technique, the complex potentials shown by Eqs. (19)–(22) are used to the region with edge crack, which is indicated by dashed line in Fig. 2. Alternatively speaking, the complex potentials shown by Eqs. (19)–(22) are used to solve the edge crack problem defined in Fig. 1.

Behaviors of the first two terms in the complex potentials are listed in Table 2. It is seen from the listed results that the first two terms can model the singular character of stress at the crack tip zone (Fig. 1). In addition, they can also model the following basic stress states: (1) $\sigma_x = c$, $\sigma_y = 0$, $\sigma_{xy} = 0$, (2) $\sigma_x = 0$, $\sigma_y \approx c$, $\sigma_{xy} = 0$ (a combination of two cases $E_1 = 1$and $F_1 = 1$in Table 2), (3) $\sigma_x = 0$, $\sigma_y = 0$, $\sigma_{xy} \approx c$, at the remote place. Since all the basic stress fields (including the pure tension and the pure shear) can be modeled by the suggested complex potentials, this is a particular advantage to use the expansion form for the short edge crack case.

In the solution, one may assume the unknowns in the following form

$$\begin{aligned} &X_{2k-1} = E_{k,re}, \quad X_{2k} = E_{k,im}, \quad X_{2N+2k-1} = F_{k,re}, \\ &X_{2N+2k} = F_{k,im}, \quad (k = 1, 2, \dots N). \end{aligned} \tag{23}$$

Similarly, the usage of the variational principle will have a solution for unknowns.

The SIFs can be defined by (Fig. 2)

$$K_1 - iK_2 = \lim_{z \to c} 2\sqrt{2\pi z}\,\phi'(z) = \frac{2\sqrt{\pi}}{\sqrt{c}} \sum_{k=1}^{N} E_k c^k. \tag{24}$$

Table 2
Behaviors of the first two terms in the complex potentials defined by Eqs. (19)–(22).

	$E_1 = 1$	$E_1 = i$	$F_1 = 1$	$F_1 = i$
The behavior of the first two terms at the crack tip zone				
σ_x	Singular stress	Regular stress	4	0
σ_y	Singular stress	Regular stress	0	0
σ_{xy}	Regular stress	Singular stress	0	0
The behavior of the first two terms at remote zone $\lvert z \rvert \gg c$ with $r = \lvert z - c \rvert$				
	$E_1 = 1$	$E_1 = i$	$F_1 = 1$	$F_1 = i$
σ_x	≈ 2	0	4	0
σ_y	≈ 2	0	0	0
σ_{xy}	0	≈ -2	0	0

From a suggested front position method (from front position of crack tip), the T-stress can be defined by [16]

$$T = \lim_{z \to c} \mathrm{Re}(\sigma_x - \sigma_y - 2i\sigma_{xy}) = 2 \lim_{z \to c} \mathrm{Re}(\Phi(z) - \overline{\Omega}(z)) = 4 \sum_{k=1}^{N} k F_{k,re} c^{k-1}. \quad (25)$$

3. Numerical examination and examples

Example 1. In the first example (Fig. 3a), we assume that the cracked rectangular plate with an edge crack has a uniform tension "p" on the tops. Two techniques are used to solve the problem. In the first case, the suggested complex potentials shown by Eqs. (19)–(22) with $c/a = 0.75$ are used, and $N = 12$ is adopted in the expansion form. In the second case, the Williams expansion form shown by Eqs. (5) and (6) is used, and $M = 24$ is adopted in the expansion form. In both cases, the number of unknowns is 48 and the series for variable "z" is up to z^{12}. In computation, we assume $h/w = 1.5$, 1.0, 0.75, 0.5, 0.4, 0.3, 0.25 (7 sets), and $a/w = 0.1$, 0.2 to 0.9 (9 sets) or $a/w = 0.01$, 0.02 to 0.09 (9 sets). The computed stress intensity factor and T-stress are expressed by

$$K_1 = F_1(a/w, h/w)p\sqrt{\pi a},$$
$$T_1 = T(1 - a/b)^2 = G(a/w, h/w)p. \quad (26)$$

In Eq. (26), T denotes the T-stress at the crack tip.

For the case of $a/w = 0.1$, 0.2 to 0.9, the computed results for $F_1(a/w, h/w)$ and $G(a/w, h/w)$ from two techniques are listed in Table 3, respectively. From the tabulated results, we see the following points. For the SIFs, if a/w ratio is small and h/w ratio is large, the discrepancy between two techniques is easily seen. For example, in the case of $a/w = 0.1$ and $h/w = 1.5$, we have $F_1 = 1.1665$ from the improved technique, and $F_1 = 1.2553$ from Williams expansion form. However, if h/w ratio is small, coincidence between two techniques has been found. For example, in the case of $a/w = 0.5$ and $h/w = 0.25$, we have $F_1 = 4.8131$ from the improved technique, and $F_1 = 4.8125$ from Williams expansion form.

For the T-stress, if a/w ratio is small and h/w ratio is large, the discrepancy between two techniques is easily seen. For example, in the case of $a/w = 0.1$ and $h/w = 1.5$, we have $G = -0.7420$ from the improved technique, and$G = -0.5932$ from Williams expansion form, and $G = -0.452$ from [5]. However, if h/w ratio is small, coincidence between two techniques has been found. For example, in the case of $a/w = 0.5$ and $h/w = 0.25$, we have $G = 1.8533$ from the improved technique, and $G = 1.8558$ from Williams expansion form, and $G = 1.858$ from [5].

For the case of $h/w = 0.5$ and $0.2 \leqslant a/w \leqslant 0.6$, comparison results for SIFs and T-stresses from various sources are listed in Table 4. From tabulated results, coincidence has been found from different techniques of solutions.

From above-mentioned results, we see that the computed results may become worse in the short edge crack case. Therefore, a computation is performed for the short crack case of $a/w = 0.01$, 0.02 to 0.09, and the computed results for $F_1(a/w, h/w)$ and $G(a/w, h/w)$ from two techniques are listed in Table 5, respectively. In Table 5, the results marked with "***" are obtained from the relevant solution in Ref. [13] for a central crack in a rectangular plate with a multiplying factor 1.1215.

From the tabulated results in Table 5, we see the following points. For the SIFs, if a/w ratio is small and h/w ratio is large, the discrepancy between two techniques is significant. For example, in the case of $a/w = 0.1$ and $h/w = 1.5$, we have $F_1 = 1.1536$ from the improved technique, and $F_1 = 2.5067$ from Williams expansion form, and $F_1 = 1.1216$ from a modified result marked with "***". However, if the h/w ratio is small and the a/w ratio is at some value, coincidence between two techniques has been found. For example, in the case of $a/w = 0.06$ and $h/w = 0.25$, we have $F_1 = 1.2653$ from the improved technique, and $F_1 = 1.2762$ from Williams expansion form.

For the T-stress, if a/w ratio is small and h/w ratio is large, the discrepancy between two techniques is significant. For example, in the case of $a/w = 0.01$ and $h/w = 1.5$, we have $G = -0.9774$ from the improved technique, and $G = -0.7648$ from Williams expansion form. From the tabulated results we found a tendency $G \to -1$ when $a/b \to 0$. However, Fett found that $G \to -0.526$ when $a/b \to 0$ [5]. Clearly, this discrepancy between different sources needs to study in detail.

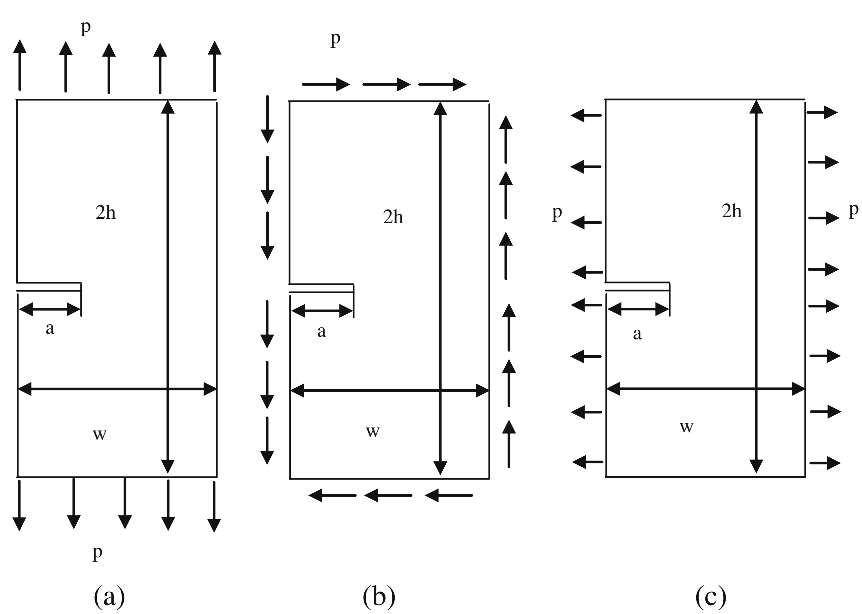

Fig. 3. Edge crack problems: (a) with tension in y-direction, (b) with shear loading, (c) with tension in x-direction.

Table 3
Non-dimensional stress intensity factor $F_1(a/w, h/w)$ and T-stress $G(a/w, h/w)$ under the tension loading "p" for an edge crack plate in the ranges: h/w = 1.5, 1.0, 0.75, 0.5, 0.4, 0.3, 0.25 and a/w = 0.1, 0.2,… to 0.9 (see Fig. 3a and Eq. (26)).

h/w a/w	1.5	1.0	0.75	0.5	0.4	0.3	0.25
Results for non-dimensional stress intensity factor $F_1(a/w, h/w)$							
0.1*	1.1665	1.1724	1.1858	1.2336	1.2838	1.3860	1.4774
0.1**	1.2553	1.2206	1.2108	1.2380	1.2844	1.3838	1.4757
0.2*	1.3598	1.3766	1.3880	1.4896	1.6282	1.9074	2.1507
0.2**	1.3813	1.3743	1.3836	1.4890	1.6282	1.9076	2.1508
0.3*	1.6658	1.6659	1.6815	1.8480	2.0737	2.5403	2.9521
0.3**	1.6649	1.6633	1.6812	1.8482	2.0735	2.5402	2.9513
0.4*	2.1147	2.1137	2.1335	2.3239	2.6049	3.2448	3.8368
0.4**	2.1107	2.1132	2.1335	2.3239	2.6049	3.2451	3.8375
0.5*	2.8142	2.8237	2.8408	3.0089	3.2955	4.0478	4.8131
0.5**	2.8109	2.8235	2.8406	3.0088	3.2956	4.0477	4.8125
0.6*	3.9803	4.0222	4.0374	4.1491	4.3780	5.1001	5.9436
0.6**	3.9675	4.0201	4.0371	4.1489	4.3784	5.1007	5.9482
0.7*	6.0883	6.2756	6.3276	6.3889	6.5142	7.0114	7.7399
0.7**	6.0303	6.2626	6.3242	6.3895	6.5137	7.0136	7.7270
0.8*	10.2857	11.2344	11.5941	11.8382	11.8901	12.0873	12.4476
0.8**	10.0468	11.1542	11.5788	11.8440	11.9189	12.1082	12.4336
0.9*	18.6088	23.9383	27.3275	31.2948	32.0406	33.0803	33.9679
0.9**	17.4891	23.2676	26.8871	30.8642	31.7383	32.9596	32.8345
Results for non-dimensional T-stress $G(a/w, h/w)$							
0.1*	−0.7420	−0.6952	−0.6512	−0.5824	−0.5475	−0.4902	−0.4438
0.1**	−0.5932	−0.5670	−0.5454	−0.5205	−0.5053	−0.4739	−0.4386
0.1***	−0.452		−0.452	−0.444	−0.432	−0.416	−0.400
0.2*	−0.5256	−0.4478	−0.4032	−0.3419	−0.2731	−0.0843	0.1386
0.2**	−0.4434	−0.4155	−0.3959	−0.3431	−0.2735	−0.0841	0.1376
0.2***	−0.374		−0.373	−0.334	−0.270	−0.084	0.143
0.3*	−0.3449	−0.3067	−0.2837	−0.1488	0.0296	0.4472	0.8893
0.3**	−0.3240	−0.3081	−0.2850	−0.1486	0.0296	0.4489	0.8915
0.3***	−0.299		−0.282	−0.148	0.030	0.449	0.890
0.4*	−0.2137	−0.2068	−0.1762	0.0397	0.3097	0.9107	1.5229
0.4**	−0.2132	−0.2074	−0.1758	0.0397	0.3095	0.9095	1.5201
0.4***	−0.208		−0.175	0.040	0.310	0.912	1.526
0.5*	−0.0977	−0.1016	−0.0695	0.1668	0.4731	1.1623	1.8533
0.5**	−0.0962	−0.1006	−0.0691	0.1670	0.4733	1.1631	1.8558
0.5***	−0.006		−0.070	0.167	0.473	1.165	1.858
0.6*	0.0314	0.0150	0.0337	0.2202	0.4904	1.1417	1.8062
0.6**	0.0372	0.0167	0.0342	0.2202	0.4904	1.1413	1.8066
0.6***	0.006		0.032	0.220	0.490	1.142	1.812
0.7*	0.1887	0.1509	0.1454	0.2361	0.4042	0.8682	1.3821
0.7**	0.1988	0.1546	0.1465	0.2362	0.4042	0.8696	1.3843
0.7***	0.122		0.134	0.234	0.404	0.869	1.387
0.8*	0.3730	0.3309	0.2985	0.2906	0.3357	0.5227	0.7857
0.8**	0.3847	0.3396	0.3029	0.2913	0.3367	0.5239	0.7727
0.8***	0.232		0.240	0.268	0.324	0.524	0.760
0.9*	0.4123	0.4921	0.5107	0.4972	0.4669	0.4515	0.4732
0.9**	0.4053	0.5005	0.5200	0.4982	0.4649	0.4480	0.4527
0.9***	0.352		0.356	0.364	0.372	0.326	0.474

* Results from the improved technique.
** Results from the Williams expansion form.
*** From Ref. [5].

Table 4
Comparison results for SIF $F_1(a/w, h/w)$ and T-stress $G(a/w, h/w)$ in the case of h/w = 0.5 and $0 \leqslant a/b \leqslant 0.9$).

a/w	$F_1(a/w, h/w)$ (h/w = 0.5)			$G(a/w, h/w)$ (h/w = 0.5)		
	*	**	***	*	**	***
0.1	1.2336	1.2380		−0.5824	−0.5205	
0.2	1.4896	1.4890	1.497	−0.3419	−0.3431	−0.3305
0.3	1.8480	1.8482	1.860	−0.1488	−0.1486	−0.1449
0.4	2.3239	2.3239	2.340	0.0397	0.0397	0.0413
0.5	3.0089	3.0088	3.033	0.1668	0.1670	0.1683
0.6	4.1491	4.1489	4.188	0.2202	0.2202	0.2218
0.7	6.3889	6.3895		0.2361	0.2362	
0.8	11.8382	11.8440		0.2906	0.2913	
0.9	31.2948	30.8642		0.4972	0.4982	

* Results from the improved technique.
** Results from the Williams expansion form.
*** From Ref. [6].

Example 2. In the second example (Fig. 3b), the cracked rectangular plate has the same configuration as in Example 1. However, the cracked plate is subjected to a shear loading "p". In this case, the mode I SIF (K_1) and T-stress are equal to zero. In computation, we assume h/w = 1.5, 1.0, 0.75, 0.5, 0.4, 0.3, 0.25 (7 sets), and a/w = 0.1, 0.2 to 0.9 (9 sets) or a/w = 0.01, 0.02 to 0.09 (9 sets). The computed stress intensity factor is expressed by

$$K_2 = F_2(a/w, h/w)p\sqrt{\pi a}. \tag{27}$$

For the case of a/w = 0.1, 0.2 to 0.9, the computed results for F_2 (a/w, h/w) from two techniques are listed in Table 6, respectively.

From the tabulated results in Table 6, we see the following points. For the SIFs, if a/w ratio is small and h/w ratio is large, some difference can be found from two techniques. For example, in the case of a/w = 0.1 and h/w = 1.5, we have F_2 = 1.2025 from the improved technique, and F_2 = 1.0547 from Williams expansion form.

Table 5
Non-dimensional stress intensity factor $F_1(a/w, h/w)$ and T-stress $G(a/w, h/w)$ under the tension loading "p" for an edge crack plate in the ranges: h/w = 1.5, 1.0, 0.75, 0.5, 0.4, 0.3, 0.25 and a/w = 0.01, 0.02,… to 0.09 (see Fig. 3a and Eq. (26)).

h/w a/w	1.5	1.0	0.75	0.5	0.4	0.3	0.25
Results for non-dimensional stress intensity factor $F_1(a/w, h/w)$							
0.01*	1.1536	1.1520	1.1503	1.1469	1.1444	1.1409	1.1390
0.01**	2.5067	2.1576	1.9498	1.7109	1.6042	1.4886	1.4336
0.01***	1.1216	1.1217	1.1218	1.1220	1.1223	1.1229	1.1235
0.02*	1.1509	1.1457	1.1407	1.1325	1.1282	1.1256	1.1271
0.02**	1.8478	1.6259	1.4997	1.3639	1.3087	1.2566	1.2356
0.02***	1.1218	1.1221	1.1225	1.1236	1.1247	1.1272	1.1296
0.03*	1.1474	1.1384	1.1311	1.1229	1.1223	1.1299	1.1403
0.03**	1.5860	1.4252	1.3380	1.2521	1.2231	1.2035	1.2025
0.03***	1.1222	1.1229	1.1239	1.1262	1.1287	1.1342	1.1396
0.04*	1.1443	1.1328	1.1253	1.1230	1.1297	1.1518	1.1738
0.04**	1.4488	1.3258	1.2628	1.2083	1.1964	1.1991	1.2117
0.04***	1.1228	1.1240	1.1257	1.1298	1.1343	1.1440	1.1535
0.05*	1.1423	1.1303	1.1250	1.1319	1.1478	1.1847	1.2183
0.05**	1.3682	1.2715	1.2249	1.1924	1.1931	1.2137	1.2391
0.05***	1.1235	1.1254	1.1280	1.1345	1.1414	1.1564	1.1712
0.06*	1.1423	1.1317	1.1302	1.1477	1.1723	1.2212	1.2653
0.06**	1.3184	1.2411	1.2064	1.1904	1.2015	1.2381	1.2762
0.06***	1.1243	1.1271	1.1309	1.1402	1.1500	1.1715	1.1925
0.07*	1.1446	1.1371	1.1399	1.1670	1.2000	1.2619	1.3170
0.07**	1.2875	1.2249	1.1990	1.1963	1.2168	1.2687	1.3197
0.07***	1.1254	1.1292	1.1343	1.1468	1.1602	1.1891	1.2173
0.08*	1.1494	1.1461	1.1532	1.1886	1.2273	1.3018	1.3686
0.08**	1.2689	1.2178	1.1987	1.2071	1.2363	1.3037	1.3677
0.08***	1.1266	1.1315	1.1382	1.1545	1.1718	1.2092	1.2455
0.09*	1.1567	1.1581	1.1687	1.2110	1.2558	1.3437	1.4204
0.09**	1.2590	1.2170	1.2031	1.2213	1.2591	1.3422	1.4200
0.09***	1.1279	1.1342	1.1426	1.1632	1.1848	1.2315	1.2766
Results for non-dimensional T-stress $G(a/w, h/w)$							
0.01*	−0.9774	−0.9746	−0.9714	−0.9648	−0.9598	−0.9519	−0.9463
0.01**	−0.7648	−0.7678	−0.7665	−0.7586	−0.7532	−0.7465	−0.7385
0.02*	−0.9512	−0.9422	−0.9329	−0.9157	−0.9046	−0.8892	−0.8788
0.02**	−0.7440	−0.7441	−0.7404	−0.7307	−0.7246	−0.7158	−0.7080
0.03*	−0.9231	−0.9072	−0.8923	−0.8675	−0.8531	−0.8341	−0.8223
0.03**	−0.7239	−0.7204	−0.7138	−0.7015	−0.6939	−0.6824	−0.6731
0.04*	−0.8945	−0.8727	−0.8535	−0.8236	−0.8071	−0.7834	−0.7674
0.04**	−0.7041	−0.6968	−0.6871	−0.6717	−0.6625	−0.6483	−0.6392
0.05*	−0.8664	−0.8399	−0.8173	−0.7824	−0.7621	−0.7311	−0.7082
0.05**	−0.6846	−0.6734	−0.6608	−0.6426	−0.6320	−0.6159	−0.6059
0.06*	−0.8394	−0.8089	−0.7829	−0.7414	−0.7161	−0.6794	−0.6510
0.06**	−0.6655	−0.6506	−0.6353	−0.6149	−0.6032	−0.5855	−0.5740
0.07*	−0.8135	−0.7794	−0.7497	−0.7008	−0.6694	−0.6249	−0.5908
0.07**	−0.6468	−0.6285	−0.6109	−0.5887	−0.5763	−0.5567	−0.5423
0.08*	−0.7888	−0.7509	−0.7167	−0.6600	−0.6262	−0.5762	−0.5378
0.08**	−0.6285	−0.6071	−0.5878	−0.5644	−0.5512	−0.5290	−0.5102
0.09*	−0.7650	−0.7229	−0.6839	−0.6202	−0.5842	−0.5301	−0.4937
0.09**	−0.6107	−0.5866	−0.5659	−0.5417	−0.5276	−0.5017	−0.4758

* Results from the improved technique.
** Results from the Williams expansion form.
*** From a technique in Ref. [13] multiplied by a factor 1.1215.

However, if h/w ratio is small, coincidence between two techniques has been found. For example, in the case of a/w = 0.5 and h/w = 0.25, we have F_2 = 1.7616 from the improved technique, and F_2 = 1.7648 from Williams expansion form.

From above-mentioned results we see that the computed results may become worse in the small edge crack case. Therefore, a computation is performed for the small crack case of a/w = 0.01, 0.02 to 0.09, and the computed results for $F_2(a/w, h/w)$ from two techniques are listed in Table 7. From the tabulated results in Table 7, we see the following points. For the SIFs, if a/w ratio is small and h/w ratio is large, the discrepancy between two techniques is significant. For example, in the case of a/w = 0.01 and h/w = 1.5, we have F_2 = 1.1560 from the improved technique, and F_2 = 2.2265 from Williams expansion form. In the semi-infinite crack with shear loading p on the interval with length "a", $K_2 = 0.9003p\sqrt{\pi a}$, or F_2 = 0.9003. Therefore, We consider that the value F_2 = 2.2265 is not reasonable.

However, if the h/w ratio is small and the a/w ratio is at some value, difference of SIFs from two techniques is not significant. For example, in the case of a/w = 0.06 and h/w = 0.25, we have F_2 = 1.1335 from the improved technique, and F_2 = 1.0851 from Williams expansion form.

Example 3. In the third second example (Fig. 3c), the cracked rectangular plate has the same configuration as in Example 1. However, the cracked plate is subjected to a tension loading "p" in x-axis direction. In this case, $K_1 = 0$, $K_2 = 0$ and T-stress is $T = p$. The same FORTRAN program used in the first example is used in the present example. In computation, we assume h/w = 1.5, 1.0, 0.75, 0.5, 0.4, 0.3, 0.25 (7 sets), and a/w = 0.1, 0.2 to 0.9 (9 sets) or

Table 6
Non-dimensional stress intensity factor $F_2(a/w, h/w)$ under the shear loading "p" for an edge crack plate in the ranges: h/w = 1.5, 1.0, 0.75, 0.5, 0.4, 0.3, 0.25 and a/w = 0.1, 0.2,… to 0.9 (see Fig. 3b and Eq. (27)).

h/w a/w	1.5	1.0	0.75	0.5	0.4	0.3	0.25
0.1*	1.2025	1.2002	1.1749	1.1221	1.1000	1.1226	1.1392
0.1**	1.0547	1.0495	1.0582	1.0814	1.0976	1.1215	1.1404
0.2*	1.1498	1.1063	1.1077	1.1456	1.1727	1.2352	1.2741
0.2**	1.0709	1.0944	1.1125	1.1465	1.1757	1.2341	1.2881
0.3*	1.1194	1.1333	1.1516	1.2048	1.2639	1.3665	1.4531
0.3**	1.1162	1.1360	1.1529	1.2091	1.2656	1.3702	1.4549
0.4*	1.1626	1.1815	1.1988	1.2855	1.3708	1.5135	1.5945
0.4**	1.1680	1.1811	1.2000	1.2867	1.3699	1.5092	1.6146
0.5*	1.2316	1.2455	1.2665	1.3748	1.4753	1.6399	1.7616
0.5**	1.2369	1.2470	1.2679	1.3749	1.4764	1.6418	1.7648
0.6*	1.3315	1.3473	1.3690	1.4750	1.5829	1.7622	1.8996
0.6**	1.3359	1.3504	1.3706	1.4758	1.5829	1.7652	1.9024
0.7*	1.4759	1.5106	1.5333	1.6153	1.7097	1.8877	2.0313
0.7**	1.4786	1.5132	1.5348	1.6156	1.7077	1.8863	2.0314
0.8*	1.6833	1.7675	1.8115	1.8732	1.9316	2.0614	2.1847
0.8**	1.6776	1.7654	1.8099	1.8721	1.9294	2.0591	2.1840
0.9*	1.9654	2.1526	2.2757	2.4177	2.4833	2.5819	2.6420
0.9**	1.9419	2.1343	2.2612	2.4064	2.4709	2.5556	2.6245

* Results from the improved technique.
** Results from the Williams expansion form.

Table 7
Non-dimensional stress intensity factor $F_2(a/w, h/w)$ under the shear loading "p" for an edge crack plate in the ranges: h/w = 1.5, 1.0, 0.75, 0.5, 0.4, 0.3, 0.25 and a/w = 0.01, 0.02,… to 0.09 (see Fig. 3b and Eq. (27)).

h/w a/w	1.5	1.0	0.75	0.5	0.4	0.3	0.25
0.01*	1.1560	1.1571	1.1583	1.1610	1.1622	1.1660	1.1739
0.01**	2.2265	1.8977	1.7116	1.5202	1.4322	1.3396	1.2725
0.02*	1.1594	1.1629	1.1668	1.1735	1.1796	1.1849	1.1946
0.02**	1.6054	1.4043	1.2968	1.1931	1.1540	1.1118	1.0894
0.03*	1.1641	1.1707	1.1772	1.1890	1.1904	1.1975	1.2006
0.03**	1.3636	1.2239	1.1552	1.0974	1.0780	1.0646	1.0622
0.04*	1.1699	1.1794	1.1881	1.1988	1.2034	1.2047	1.1895
0.04**	1.2387	1.1381	1.0936	1.0630	1.0564	1.0585	1.0605
0.05*	1.1761	1.1879	1.1962	1.2028	1.1971	1.1790	1.1733
0.05**	1.1660	1.0933	1.0653	1.0527	1.0553	1.0636	1.0752
0.06*	1.1823	1.1955	1.2020	1.1968	1.1815	1.1543	1.1335
0.06**	1.1210	1.0688	1.0528	1.0529	1.0605	1.0758	1.0851
0.07*	1.1887	1.2012	1.2040	1.1815	1.1577	1.1269	1.0761
0.07**	1.0919	1.0561	1.0491	1.0580	1.0694	1.0875	1.1022
0.08*	1.1942	1.2040	1.1987	1.1611	1.1338	1.0995	1.0970
0.08**	1.0736	1.0501	1.0497	1.0652	1.0785	1.0986	1.1114
0.09*	1.1991	1.2042	1.1896	1.1411	1.1152	1.1217	1.0928
0.09**	1.0618	1.0484	1.0533	1.0733	1.0886	1.1100	1.1279

* Results from the improved technique.
** Results from the Williams expansion form.

a/w = 0.01, 0.02 to 0.09 (9 sets). By using the two above-motioned techniques, the computed results coincide with the exact solution, or $K_1 = 0$, $K_2 = 0$ and T-stress is $T = p$. As claimed previously, the first two leading terms in the Williams expansion form have the stress state $\sigma_x = c$, $\sigma_y = 0$ and $\sigma_{xy} = 0$ at remote place. Therefore, it is not strange to find a coincidence between two techniques.

4. Conclusions

In the present study, one needs to approximate a real stress field by a linear combination of many basic stress fields, which satisfy the traction free condition along the crack face in advance. It is seen that the results obtained in the solution of the edge crack problem must depend on the adopted basic stress fields. In fact, a linear combination of the complex potentials shown by Eqs. (5) and (6) will formulate the complex potentials shown by Eqs. (19)–(21). However, this linear combination is expressed in the form of an infinite series. In a real computation, we have to truncate final terms in computation. Therefore, it is natural to obtain the different numerical results when different complex potentials are used. A detailed computation finds that the Williams expansion may not be suitable for the case of short edge cracks.

It is expected that the EEVM provides a reasonable way to solve the edge crack problem, since it does not depend on the collocation scheme adopted. In addition, the EEVM is based on the least potential energy principle in elasticity. That is to say the numerical results obtained from the EEVM is the optimum one from the viewpoint of the least potential energy principle in elasticity.

5. Discussions

We can explain the studied problem from theory of function approximation. It is known that the function approximation is an important topic in the numerical analysis. Generally, the given function is approximated by a linear combination of many basic functions. The following is a simple example. Suppose the given function is defined by

$$f(x) = \cos x \quad (-\pi \leqslant x \leqslant \pi). \tag{28}$$

In the first case, the function is approximated by a Fourier series, and the approximated function is denoted by $f_p(x)$. In this case, we have

$$f_p(x) = \cos x, \quad f(x) = f_p(x) \quad (-\pi \leqslant x \leqslant \pi). \tag{29}$$

In the second case, the function is approximated by a polynomials, and the approximated function is denoted by $f_q(x)$. If truncating three terms in the series expansion, we can obtain

$$f_q(x) = 1 - 0.472832x^2 + 0.027376x^4, \quad f(x) \neq f_q(x) \quad (-\pi \leqslant x \leqslant \pi). \tag{30}$$

In this case, we have $\max|f(x) - f_q(x)| = 0.09$ and the deviation is not small.

From the above-mentioned results, it is not strange to meet a similar situation in the edge crack problem using expansion form.

Acknowledgement

The project was supported by National Natural Science Foundation of China.

References

[1] M.L. Williams, ASME J. Appl. Mech. 24 (1957) 111–114.
[2] J.R. Rice, J. Mech. Phys. Solids 22 (1974) 17–26.
[3] T.L. Sham, Int. J. Fract. 48 (1991) 81–102.
[4] T. Fett, Eng. Fract. Mech. 57 (1997) 365–373.
[5] T. Fett, Eng. Fract. Mech. 60 (1998) 631–652.
[6] B. Yang, K. Ravi-Chandar, Eng. Fract. Mech. 64 (1999) 589–605.
[7] X. Wang, Eng. Fract. Mech. 69 (2002) 1339–1352.
[8] Q.Z. Xiao, B.L. Karihaloo, Eng. Fract. Mech. 69 (2002) 959–981.
[9] C.L. Tan, X. Wang, Eng. Fract. Mech. 70 (2003) 2247–2252.
[10] W.K. Wilson, J. Basic Eng. 93 (1971) 685–690.
[11] J.T. Chen, Y.T. Lee, S.R. Yu, S.C. Shieh, Eng. Anal. Bound. Elem. 33 (2009) 678–688.
[12] Y.Z. Chen, Eng. Fract. Mech. 17 (1983) 387–394.
[13] Y.Z. Chen, X.Y. Lin, Z.X. Wang, Fatigue Fract. Eng. Mater. Struct. 31 (2008) 478–487.
[14] N.I. Muskhelishvili, Some Basic Problems of Mathematical Theory of Elasticity, Noordhoff, Leyden, 1963.
[15] Y.Z. Chen, N. Hasebe, K.Y. Lee, Multiple Crack Problems in Elasticity, WIT Press, Southampton, 2003.
[16] Y.Z. Chen, Z.X. Wang, X.Y. Lin, J. Mech. Mater. Struct. 3 (2008) 1659–1673.